IEEE IST 2005
International Workshop on Imaging Systems and Techniques
Niagara Falls, Sheraton Hotel on the Falls, 13-14 May 2005

Construction of a Computational Non-Planar Curved Tube Model from MRI Data

Thomas A. Spirka[1], Jerry G. Myers[2], Randolph M. Setser[1,3], Sandra S. Halliburton[1,3], Richard D. White[3], George P. Chatzimavroudis[1,3]
[1]Department of Chemical and Biomedical Engineering, Cleveland State University, Cleveland, OH
[2]NASA - Glenn Research Center, Exploration Systems Division, Cleveland, OH
[3]Division of Radiology, The Cleveland Clinic Foundation, Cleveland, OH

Abstract *– The construction of computational models from images of experimental or clinical vascular models should result in more reliable flow simulations, but it is accompanied by great challenges. Curvature, branching, and the lack of planarity in a model are some of the factors that complicate both the imaging procedure and the image data processing performed in order to extract the geometry and re-construct the models. This study describes the methodology developed to image and construct a computational model of an non-planar aortic arch glass model to be used for simulations of blood flow.*

Keywords *– Computational fluid dynamics, magnetic resonance imaging, aortic arch*

I. INTRODUCTION

Recent studies investigating the role of blood flow in the development and progression of atherosclerosis have reported imaging protocols and image processing methods for constructing computational models of arterial geometries. Many of these studies have focused on the carotid bifurcation [1-6], whereas others focused on the abdominal aorta bifurcation [7-9] have focused on the bifurcation of the abdominal aortic artery into the iliac arteries. A few studies have focused on the ascending [10] and descending aorta [11].

Most of the previous studies constructed the computational models from a series of transverse magnetic resonance imaging (MRI) or computed tomography (CT) slices. The geometric information obtained from these slices was extracted through the use of a snake algorithm or a thresholding segmentation algorithm. The imaging methods used work well when the geometry to be constructed as a model is either planar or very close to planar. However, these methods have problems when the geometry to be modeled is non-planar in orientation, as in the case of the aortic arch. The difficulty in this case occurs during the construction of the portion of the geometry that connects the ascending and descending vessels of the aortic arch. The focus of this paper is to present a method that uses a series of oblique transverse and oblique sagittal MRI slices to construct a computational model of a simplified aortic arch experimental glass model.

II. METHODOLOGY

A. Model and Experimental Setup

The experimental model of the aortic arch (Fig.1) was made of glass (Technical Glass Products Inc., Painesville, OH) and it was constructed based on the typical literature dimensions with certain simplifications. The inner diameter was constant throughout the length of the model and equal to 25.4 mm. The model was non-planar at the arch such that there was a 20-degree angle between the ascending and descending straight parts. The arch had a radius of curvature equal to 19.04 mm. No branches were included at the top of the arch to focus on the non-planarity only. The model was mounted inside a polycarbonate box which was filled with water.

(a) (b)

Figure 1 - Schematic of the aortic arch model used (not to scale): (a) top view; (b) side view

The model was connected to a flow loop. A ¼ hp pump (Flotec, Delavan, WI) was used to provide steady flow throughout the flow loop. The flow rate was controlled through the use of a valve set distal to the pump in the flow loop and was set and monitored using a rotameter (Dakota Instruments, Orangeburg, NY) placed in-line after the valve in the loop. A flow rate of 3.0 L/min (Reynolds Number = 2930) was used during the acquisition of the images required to construct the computational model of the model.

B. *MRI Procedure*

The aortic arch phantom was scanned in a 1.5 Tesla MRI scanner (Sonata, Siemens Medical Solutions, Erlangen, Germany) under steady flow conditions. Several imaging protocols were tested, including true-FISP, and traditional gradient-echo, in order to determine the protocol that would best visualize the model. It was determined that a gradient echo (bright blood) imaging protocol produced the clearest images. To obtain the necessary geometric data for the ascending and descending portion of the model, a series of 20 contiguous, 5 mm thick, slices were placed perpendicular to the long axis of the ascending portion of the model. The arch was imaged with a series of oblique transverse/oblique sagittal slices. This oblique slices were placed by first setting a transverse slice perpendicular to the long axis of the ascending part of the model (base of the arch) and then rotating it. The axis of rotation was an anterior-to-posterior line passing through the center of the original transverse slice in the left-to-right direction. By sequentially rotating the slice around this rotation axis in a clockwise direction, 35 images, separated by 5 degrees, were acquired with a slice thickness of 3 mm encompassing a total rotation of 180 degrees to cover the entire arch and obtain the necessary geometric information. The MRI settings for both sets of images are shown in Tables 1 and 2. Fig.2 illustrates the position of the slices required to obtain the geometric information.

Table 1:
MRI parameters for the transverse images

Number of Slices	20
Distance between Slices	0 mm
Slice Orientation	Transverse
Field of View	256x256 mm^2
Slice Thickness	5mm
TR	26 ms
TE	8.1 ms
Matrix Size	256x256
# of Signal Averages	4
Voxel Size	1mm x 1mm x 5mm

It should be noted that the angle of the slice in relation to the original transverse slice determined whether the image was considered oblique transverse or oblique sagittal. If the angle of the slice was ≤ 45 degrees, or ≥ 135 degrees, then the slice was oblique transverse in orientation. If the angle of the slice was > 45 degrees but < 135 degrees, then the slice was oblique sagittal in orientation. If the angle of the slice was 90 degrees to the original slice, then the slice was sagittal in orientation.

Table 2:
MRI parameters of the oblique images

Number of Slices	35
Distance between Slices	0 mm
Slice Orientation	Oblique Transverse or Oblique Sagital
Field of View	256x256 mm^2
Slice Thickness	3 mm
TR	26 ms
TE	8.1 ms
Matrix Size	256x256
# of Signal Averages	4
Voxel Size	1mm x 1mm x 3mm

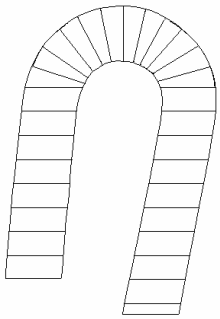

Figure 2 – Positioning of the imaging slices for the aortic arch model

C. *Image Processing*

The images with the geometric information were processed using the freeware DICOM viewing software ImageJ (National Institute of Health, Bethesda, MD) along with the plug-in Spline Snake (Matthews Jacob, University of Illinois at Urbana Champaign). The Spline Snake plug-in extracted the X and Y coordinates of a curve corresponding to the edge of the lumen of the model by using a snake algorithm [12]. In this algorithm, the energy function of an initial closed curve set by the user was minimized as the curve deformed and moved like a snake, until the location and shape of the curve corresponded to the location and shape of the boundary curve (the interface between lumen and wall). The Spline Snake plug-in generated a list of X and Y coordinates of this final curve. The origin of the coordinate system was located at the top left hand corner of the image and all coordinates were determined using this point as the reference. In order to position these coordinates in the three-dimensional space, the user had to modify the coordinate system by adding the Z coordinate and accounting for the angle and location of each individual slice.

D. *Model Construction*

The X, Y, and Z coordinates generated for each segmented curve were imported into the three-dimensional modeling software package Rhinoceros (Robert McNeel & Associates, Seattle, WA) as point clouds. The use of point clouds allowed all of the points associated with a particular curve to be imported at the same time, while maintaining their relationship to one another. A non-uniform rational B-spline (NURBS) was then fit to the imported coordinates using the individual coordinates as control points for the NURBS. A NURBS was fit to each set of coordinates corresponding to each boundary segmented using the Spline Snake plug-in. Once all of the curves were imported (Fig.3), all of the curves were smoothed using a smoothing algorithm provided by Rhinoceros. The smoothing step was required to remove the roughness of the curves caused by partial volume effects and pixelation of a rounded image. After smoothing, a NURBS surface was constructed from the curves by lofting a surface over the curves (Fig.4). The use of the oblique transverse and oblique sagittal images allowed the surface of the entire phantom to be created in a single step, because the curves provided the software with a logical lofting path to build the surface; this would not be the case when only transverse images were used (Fig.5 and Fig.6).

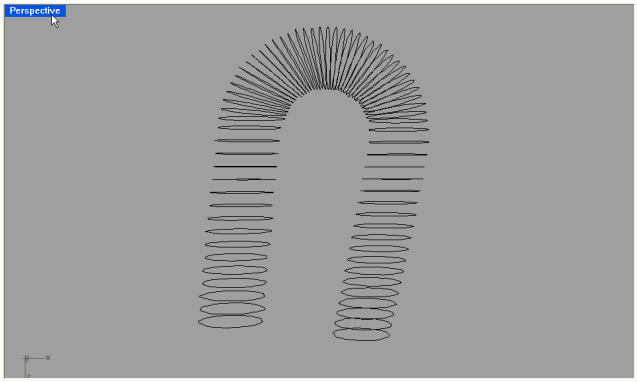

Figure 3 - Imported curves

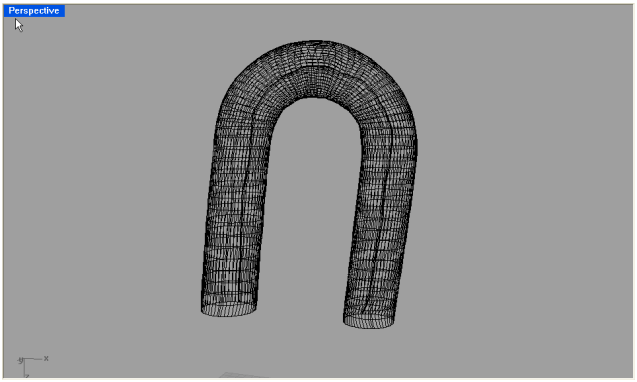

Figure 4 - Lofted NURBS surface

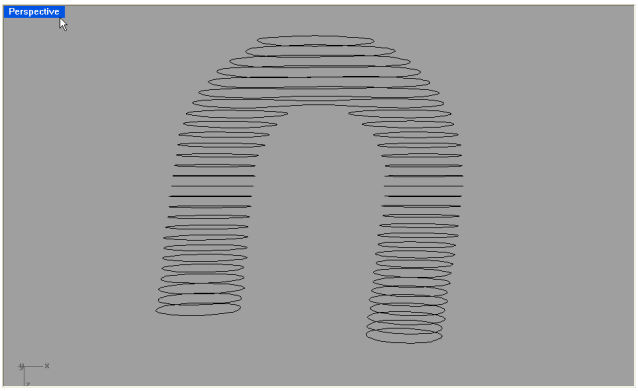

Figure 5 - Imported transverse curves

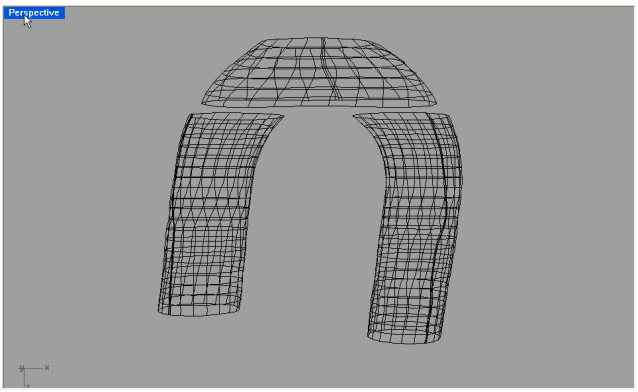

Figure 6 - Lofted NURBS surface using only transverse curves

When only transverse curves were used, a total of three surfaces were created by using three separate lofting steps. The reason for this is that, as the software reached the top of either the ascending or descending portions of the model, there was no logical direction in which to proceed. The lofting tool essential had to loft a surface in two directions (a task not possible using this software). The process could be completed only by plotting additional points to construct the bottom of the arch and constructing a surface by hand to join the three lofted surfaces and close the top of the arch. This problem was eliminated by using the oblique curves.

III. RESULTS AND DISCUSSION

Measurements of the diameter of the straight sections of the phantom were obtained through the use of a telescoping gauge and a micrometer. The results were compared to the corresponding diameter of the computational model which was determined by calculating the cross-sectional area of the corresponding section using a feature in Rhinoceros. The apparent diameter of the cross-section was then calculated.

The diameter of the computational model agreed with the measured diameter in all cases to within 1.0 mm. The ultimate use for the models created with this method was to conduct flow simulations using commercial computational fluid dynamics (CFD) software packages and to compare the CFD velocity findings with experimental MRI velocity measurements. After completion of the flow simulations, it was found that the MRI-measured local velocities differed from the CFD-predicted velocities by less than 2 cm/s on average

IV. CONCLUSION

This paper described the procedure to reconstruct a computational model of an experimental glass phantom of the aortic arch. The reconstruction was successful when a combination of transverse and oblique images was used in order to help the modelling software in the lofting procedure. The resulting computational model was geometrically and fluid mechanically in agreement with the glass model.

REFERENCES

[1] D. A. Steinman, "Image based computational fluid dynamics modeling in realistic arterial geometries". *Ann. Biomed. Eng.*, Vol. 30, pp. 493-97, 2002.

[2] D. A. Steinman, J. B. Thomas, H. M. Ladak, J. S. Milner, B. K. Rutt, J.D. Spence, "Reconstruction of carotid bifurcation hemodynamics and wall thickness using computational fluid dynamics and MRI". *Magn. Res. Med.*, Vol. 47, pp. 149-59, 2002.

[3] Q. Long, X. Y. Xu, B. Ariff, S. A. Thom, A. D. Hughes, A. V. Stanton, "Reconstruction of blood flow patterns in a human carotid bifurcation: a combinded CFD and MRI study". *JMRI*, Vol. 11. pp. 299-311, 2000 .

[4] R. Botnar, G. Rappitsch, M. B. Scheidegger, D. Liepsch, K. Perktold, P. Boesiger, "Hemodynamics in the carotid artery bifurcation: A comparison between numerical simulations and in-vitro MRI measurements". *J. Biomech.*, Vol. 33, pp. 137-44, 2000.

[5] S. Z. Zhao, X. Y. Xu, A. D. Hughes, S. A. Thom, A. V. Stanton, B. Ariff, Q. Long, "Blood flow and vessel mechanics in a physiologically realistic model of a human carotid arterial bifurcation". *J. Biomech.* Vol. 33, pp. 975-84, 2000.

[6] I. Marshall, S. Zhao, P. Papathanasopoulou, P. Hoskins, X. Y. Xu, "MRI and CFD studies of pulsatile flow in healthy and stenosed carotid bifurcation models". *J. Biomech.*, Vol. 37, pp. 679-87, 2004.

[7] Q. Long, X.Y. Xu, M. Bourne, and T. M. Griffith Numerical study of blood flow in an anatomically realistic aorto-iliac bifurcation generated from MRI data". *Magn. Res. Med.*, Vol. 43, pp. 565-76, 2000.

[8] J. A. Moore, B. K. Rutt, S. J. Karlik, K. Yin, C. R. Ethier, "Computational blood flow modeling based on in vivo measurements". *Ann. Biomed. Eng.*, Vol. 27, pp. 627-640, 1999.

[9] M. Bonert, R. L. Leaskl, J. Butany, R. Ethier, J. G. Myers, W. Johnston, M. Ojha, "The relationship between wall shear stress distributions and intimal thickening in the human abdominal aorta". *BioMed. Eng. Online*, Vol. 2:18, 2003. (http://www.biomedical-engineering-online.com).

[10] N. B. Wood, S. J. Weston, A. D. Gosman, D. N. Firmin, "Combined MR imaging and CFD simulation of flow in the human descending aorta". *JMRI*, Vol. 13, pp. 699-713, 2001.

[11] A. Leuprecht, S. Kozerke, P. Boesiger, K Perktold, "Blood flow in the human ascending aorta: a combined MRI and CFD study". *J. Eng. Math.*, Vol. 47, pp. 387-404, 2003.

[12] M. Jacob, T. Blu, M. Unser, "Efficient energies and algorithms for parametric snakes". *IEEE Trans. Image Proc.*, **13**, Vol. 13, pp. 1231-44, 2003.